Capacity Analysis of Uplink Multi-user SC-FDMA System With Frequency-Dependent I/Q Imbalance

Aamir Ishaque, Pranav Sakulkar and Gerd Ascheid
*Institute for Communication Technologies and Embedded Systems, RWTH Aachen University, Germany
Email: {ishaque,sakulkar,ascheid}@ice.rwth-aachen.de

***Abstract*—In this paper, we investigate the capacity of the multi-user (MU) channels with the single-carrier frequency-division-multiple-access (SC-FDMA) transceivers using widely linear equalizers (WLE) to counteract front-end I/Q imbalance (IQI) issues. When the erroneous channel knowledge is available at the equalizer, it is shown that the mutual information could be expressed as a function of the eigenvalues of the direct and image channel realization. Expressions for the error variance of the effective channel and the associated channel capacity are derived in closed form and discussed under special cases. Numerical analysis shows that the ergodic and outage capacity of WLE receivers tends to achieve a capacity region in the vicinity of an ideal system and considerably extends the coverage region of the cell. The impact of the channel correlation and the IQI on the outage probability is also investigated, which highlights the crucial role of the MU resource assignment in exploiting the spectral diversity and their optimality in the presence of IQI.**

I. Introduction

A major challenge in the modern uplink communication is the realization of the efficient high-data rate links through multi-path channels and relaxed requirements on the power amplifiers of the transmitter. The waveforms, therefore, need to have multi-carrier functional blocks but a lower peak-to-average-power ratio as compared to the conventional OFDM systems, whereas the device analogue implementation should produce minimal distortion. Single carrier frequency division multiple access (SC-FDMA) has been adopted in 3GPP LTE standard as an uplink waveform [1], since it enjoys higher power efficiency suitable for mobile handsets and a simple frequency-domain equalization, in addition to offering flexibility in multi-user (MU) resource sharing.

In low cost terminals, the radio front-ends inevitably suffer from analogue imperfections that are unpredictable and vary from device to device. Recently, one of the frequency-conversion method of choice has been *zero-IF* radio architectures due to their high integrability and low complexity [2]. However, their implementation suffer from a number of impairments; the major source of degradation being the mismatch between the I and Q chains during the quadrature conversion phase. In a multi-carrier system, it appears as the interference from the mirror subcarrier that motivates the I/Q imbalance (IQI) suppression using, **a)** *IQI cancellation*, if IQI is small and non-frequency dependent (NFD) [3], [4], or **b)** *pair-wise equalizers* [5], [6], otherwise. In [7], the pilot design problem was studied for the dual-channel estimation necessary for the pair-wise equalizers. An information theoretic perspective of the IQI problem was provided in [8], where the channel correlation and the IQI were shown to strongly influence the outage capacity. However, the perfect channel knowledge and the ideal channel equalization were assumed. It was shown in [9] that an SC-FDMA system achieves full diversity gain with a hybrid subcarrier assignment scheme [10].

Our aim in this paper is to investigate the limits on the uplink MU SC-FDMA communication enforced by the erroneous channel estimation and the impaired front-end I/Q processing. In this context, we make the following contributions:

- Compute the error variance of the channel estimator that is an extension of the pilot-aided technique [7] to MU scenario and based on the linear minimum mean square error (LMMSE) criterion.
- We derive the lower bound on the average user sum-capacity, when IQI is suppressed with *widely linear equalizers* (WLE) [11]. Asymptotic behavior and the optimal transmit power allocation scheme given the partial channel knowledge and the receiver structure are also discussed.
- Outage probability is provided in a closed-form that matched closely with the experimental results and gives some important insights into the channel correlation effects on the MU achievable capacity with outage constraint.
- Numerical examples illustrate the diversity gain achieved by various subcarrier assignment schemes and the role of avoiding inter-user interference due to the IQI in the outage performance.

The remainder of the paper is organized as follows. In Section II, a mathematical description of the investigated MU system is provided, along with the influence of joint transmitter and receiver FD IQI. This is followed by the compensation method using WLEs and a channel estimation error model using specifically designed pilots tones. Ergodic and outage capacity computation is targeted in Section III. Using Monte Carlo simulation framework, Section IV subsequently presents the capacity results obtained with and without I/Q imbalance compensation and studies the residual capacity degradation w.r.t an ideal system. Finally, Section

V draws some conclusions and highlights the main outcome of this study.

Notation: Vectors are represented by lower-case and matrices by upper-case boldface letters. $(\cdot)^T$, $(\cdot)^*$ and $(\cdot)^H$ denote transpose, conjugation and conjugate-transpose operations respectively; $\mathbf{I}$ and $\mathbf{0}$ represent the identity and null matrices respectively; $\mathrm{Tr}\{\cdot\}$, $\mathbb{E}\{\cdot\}$, $\mathrm{var}\{\cdot\}$ and $\mathrm{cov}\{\cdot,\cdot\}$, refer to trace, expectation, variance and covariance operators respectively; $\otimes$ denotes the linear convolution; $\mathcal{CN}(\boldsymbol{\mu},\boldsymbol{\Sigma})$ stands for complex Gaussian random vectors with mean $\boldsymbol{\mu}$ and covariance matrix $\boldsymbol{\Sigma}$; $\mathrm{diag}_n\{\cdot\}$ provides n-th diagonal of the argument matrix whereas $\mathrm{cric}\{\cdot\}$ creates a circulant matrix from the argument vector.

II. System Model

Let us consider an uplink MU communication system with a single sector employing SC-FDMA. Assume K active users indexed by $\mathcal{K}=\{1,2,\ldots,K\}$ are scheduled at a given instant. They use equal spectral resources indexed by the sub-channels $\mathcal{S}_k=\{s_{k,1},s_{k,2},\ldots,s_{k,M}\}$ for transmission over a multi-path channel $\boldsymbol{h}_k$ of length L. The ideal transmit signal of the k-th user can be described by M elements of

$$\boldsymbol{u}_k=\mathbf{F}_N^H\mathbf{S}_k\mathbf{F}_M\boldsymbol{x}_k \tag{1}$$

where $\mathbf{F}_Q$ denoted Q-point FFT matrix. The $N\times M$ mapping matrix $\mathbf{S}_k$ obeys exclusivity constraint i.e., the subcarrier allocation set follows $\mathcal{S}_k\cap\mathcal{S}_l=\emptyset,\ \forall\ k\neq l$. The complex signal undergoes RF processing, whose output suffers from frequency-dependent (FD) IQI modeled here as follows

$$\tilde{\boldsymbol{u}}_k=\boldsymbol{g}_{1T,k}\otimes\boldsymbol{u}_k+\boldsymbol{g}_{2T,k}\otimes\boldsymbol{u}_k^* \tag{2}$$

where the transmit IQI is represented by two complex vectors given by

$$\boldsymbol{g}_{1T,k}=\alpha_{T,k}\boldsymbol{a}_{T,k}+\beta_{T,k}\boldsymbol{b}_{T,k} \tag{3}$$

$$\boldsymbol{g}_{2T,k}=\alpha_{T,k}\boldsymbol{b}_{T,k}+\beta_{T,k}\boldsymbol{a}_{T,k} \tag{4}$$

for NFD IQI parameters $\{\epsilon_{T,k},\phi_{T,k}\}$ so that $\alpha_{T,k}=\cos(\phi_{T,k})+j\epsilon_{T,k}\sin(\phi_{T,k})$ and $\beta_{T,k}=\epsilon_{T,k}\cos(\phi_{T,k})+j\sin(\phi_{T,k})$, and FD part is given by $\boldsymbol{a}_{T,k}=\left(\boldsymbol{g}_{T,k}^I+\boldsymbol{g}_{T,k}^Q\right)/2$ and $\boldsymbol{b}_{T,k}=\left(\boldsymbol{g}_{T,k}^I-\boldsymbol{g}_{T,k}^Q\right)/2$, where $\boldsymbol{g}_{T,k}^I$ and $\boldsymbol{g}_{T,k}^Q$ are real-valued I and Q channel gains with L_T non-zero entries. The received signal block under receiver IQI is obtained as follows

$$\begin{aligned}\boldsymbol{r}=\sum_{k=1}^{K}&\underbrace{\left(\boldsymbol{g}_{1R}\otimes\boldsymbol{h}_k\otimes\boldsymbol{g}_{1T,k}+\boldsymbol{g}_{2R}\otimes\boldsymbol{h}_k^*\otimes\boldsymbol{g}_{2T,k}^*\right)}_{=:\boldsymbol{h}_{1,k}}\otimes\boldsymbol{u}_k\\&+\underbrace{\left(\boldsymbol{g}_{1R}\otimes\boldsymbol{h}_k\otimes\boldsymbol{g}_{2T,k}+\boldsymbol{g}_{2R}\otimes\boldsymbol{h}_k^*\otimes\boldsymbol{g}_{1T,k}^*\right)}_{=:\boldsymbol{h}_{2,k}}\otimes\boldsymbol{u}_k^*+\tilde{\boldsymbol{n}}\end{aligned} \tag{5}$$

where $\tilde{\boldsymbol{n}}=\boldsymbol{g}_{1R}\otimes\boldsymbol{n}+\boldsymbol{g}_{2R}\otimes\boldsymbol{n}^*$, $\boldsymbol{n}\sim\mathcal{CN}(\mathbf{0},\sigma_n^2\mathbf{I})$, $\boldsymbol{g}_{1R}=\alpha_R\boldsymbol{a}_R+\beta_R^*\boldsymbol{b}_R$, $\boldsymbol{g}_{2R}=\alpha_R^*\boldsymbol{b}_R+\beta_R\boldsymbol{a}_R$ and parameters $\{\alpha_R,\beta_R,\boldsymbol{a}_R,\boldsymbol{b}_R\}$ defined similar to TX representations. Entries of $\boldsymbol{h}_k$ are independent and identically distributed (i.i.d.) zero-mean circularly symmetric complex Gaussian random variables (RVs) with power delay profile given as $\mathbf{R}_{\boldsymbol{h}_k}$ and $\{\boldsymbol{h}_k\}_{k=1}^K$ are assumed as stationary and ergodic RVs. After the CP removal and the analysis filters, the per-user received signal is extracted from $\boldsymbol{r}$ using the associated assignment matrix $\mathbf{S}_k$. The I/O relationship with the penultimate iFFT operation provides the k-th user signal as

$$\boldsymbol{y}_k=\boldsymbol{\Lambda}_{1,k}\boldsymbol{x}_k+\boldsymbol{\Lambda}_{2,k'}\tilde{\boldsymbol{x}}_{k'}+\tilde{\boldsymbol{n}}_k \tag{6}$$

where $\tilde{\boldsymbol{x}}_k=\mathbf{F}_M^H\mathbf{F}_M^*\boldsymbol{x}_k^*$, $\boldsymbol{\Lambda}_{i,k}=\mathbf{F}_M^H\mathbf{S}_k^T\mathbf{F}_N\mathrm{circ}\{\boldsymbol{h}_{i,k}\}\mathbf{F}_N^H\mathbf{S}_k\mathbf{F}_M$ is a $M\times M$ circulant matrix with the first column given as $\bar{\boldsymbol{\lambda}}_{i,k}=[\bar{\lambda}_{k,1}^{(i)},\bar{\lambda}_{k,2}^{(i)},\ldots,\bar{\lambda}_{k,M}^{(i)}]$, $\tilde{\boldsymbol{\lambda}}_{i,k}=\mathbf{F}_M\bar{\boldsymbol{\lambda}}_{i,k}$ and $i=\{1,2\}$.

A. Widely-Linear Equalizers

To gain additional degrees of freedom and improve receiver performance, the optimal linear solution is to exploit signal properties for synthesizing the channel equalizers that operate over both the received observation $\boldsymbol{r}$ and its conjugate $\boldsymbol{r}^*$. Non-circularity property of the transmitted constellation symbols $\boldsymbol{x}_k$ provides just such an additional knowledge [11]. However, as the circular modulation schemes (e.g., M-PSK and M-QAM) have been widely adopted in the current standards, in this paper we instead use the inter-relationship between $\boldsymbol{y}_k$ and $\boldsymbol{y}_{k'}^*$ to estimate an IQI-effected signal, that could lead to some performance enhancement depending on the strength of IQI coefficients $\bar{\boldsymbol{\lambda}}_{2,k}$. The symbol estimates correspond to

$$\hat{\boldsymbol{x}}_k=\mathbf{G}_{1,k}\boldsymbol{y}_k+\mathbf{G}_{2,k}\boldsymbol{y}_{k'}^* \tag{7}$$

where k'-th user occupies image band of user-k such that $\mathcal{S}_{k'}=N-\mathcal{S}_k$. In an OFDM-based system, this approach is equivalent to the pair-wise equalizers proposed for compensating IQI in the single-user systems [6]. From (6), we have

$$\boldsymbol{y}_{k;k'}=\mathbf{H}_{k;k'}\boldsymbol{x}_{k;k'}+\boldsymbol{w}_{k;k'} \tag{8}$$

$\boldsymbol{y}_{k;k'}=[\boldsymbol{y}_k^T\boldsymbol{y}_{k'}^H]^T$, $\boldsymbol{x}_{k;k'}=[\boldsymbol{x}_k^T\boldsymbol{x}_{k'}^H]^T$, where the *effective* channel $\mathbf{H}_{k;k'}$ is given by

$$\mathbf{H}_{k;k'}=\begin{pmatrix}\boldsymbol{\Lambda}_{1,k} & \boldsymbol{\Lambda}_{2,k'}\\ \boldsymbol{\Lambda}_{2,k}^* & \boldsymbol{\Lambda}_{1,k'}^*\end{pmatrix}. \tag{9}$$

B. Channel Estimation

To construct the widely-linear equalizers (7), one needs the estimates of the direct $\bar{\boldsymbol{\lambda}}_{1,k}$ and the image $\bar{\boldsymbol{\lambda}}_{2,k}$ channels. We employ a training sequence aided approach for MU channel estimation.[1] After user separation and CP removal, we can rewrite (5) for the k-th user as

$$\boldsymbol{r}_k=\mathbf{U}_k\boldsymbol{h}_{1,k}+\mathbf{U}_{k'}^*\boldsymbol{h}_{2,k}+\tilde{\boldsymbol{n}}_k \tag{10}$$

where $\mathbf{U}_k$ is a circulant matrix with the first column as $\boldsymbol{u}_k=[u_{k,1},u_{k,2},\ldots,u_{k,N}]^T$. The training symbols are designed in such a manner that the direct and image channels are decoupled and it is assumed that the effective channels $\boldsymbol{h}_{i,k}$ satisfy identifiability condition, i.e., $L\leq M/2$ [7], where the

[1] In LTE standard, all users simultaneously transmit a preamble block every 4^{th} symbol block of an uplink time-slot [12].

channel $\boldsymbol{h}_{i,k}(l)$ is shortened for $L_R + L + L_T \geq l > L$ due to weak FD IQI taps. In general, the following conditions should be satisfied: $\mathbf{U}_k^H \mathbf{U}_k = P_T \mathbf{I}$, $\mathbf{U}_k^H \mathbf{U}_l^* = \mathbf{0}\ \forall\ k, l$ and $\mathbf{U}_k^H \mathbf{U}_l = \mathbf{0},\ \forall\ l \neq k$, which imply that the pilot tones must be equi-spaced, equi-powered and the image tones must be set to zero. The LMMSE estimator of $\boldsymbol{h}_{i,k}$ is given by

$$\hat{\boldsymbol{h}}_{i,k} = \mathbf{R}_{\boldsymbol{h},\boldsymbol{r}}^{(i)} \mathbf{R}_{\boldsymbol{r}}^{-1} \boldsymbol{r}_k \tag{11}$$

where $\mathbf{R}_{\boldsymbol{h},\boldsymbol{r}}^{(i)} = \mathbb{E}\left\{\boldsymbol{h}_{i,k}\boldsymbol{r}_k^H\right\} = \mathbf{R}_{\boldsymbol{h}}^{(i)}\mathbf{U}_k^H$ and $\mathbf{R}_{\boldsymbol{r}} = \mathbb{E}\left\{\boldsymbol{r}_k\boldsymbol{r}_k^H\right\} = \mathbf{U}_k\mathbf{R}_{\boldsymbol{h}}^{(i)}\mathbf{U}_k^H + \mathbf{R}_{\tilde{\boldsymbol{n}}}$. Note that due to TX/RX IQI, $\boldsymbol{h}_{i,k}$ deviates from $\boldsymbol{h}_k$ and the distribution of $\boldsymbol{h}_{i,k}$ is a function of IQI parameters. Fortunately, the estimate of the effective channel correlation inherently incorporates the effects of IQI and the correlation matrix $\mathbf{R}_{\boldsymbol{h}_k}$ is irrelevant in our scenario. Furthermore, if the receiver IQI is small (generally the case), the noise samples are uncorrelated i.e., $\mathbf{R}_{\tilde{\boldsymbol{n}}} = \mathbb{E}\left\{\tilde{\boldsymbol{n}}_k\tilde{\boldsymbol{n}}_k^H\right\} \approx \sigma_n^2\mathbf{I}$. The error covariance matrix for $\boldsymbol{e}_{i,k} = \hat{\boldsymbol{h}}_{i,k} - \boldsymbol{h}_{i,k}$ is i.i.d. Gaussian distributed and given by

$$\mathbf{R}_{\boldsymbol{e}}^{(i)} = \left(\mathbf{R}_{\boldsymbol{h}}^{(i)^{-1}} + \rho_T\mathbf{I}\right)^{-1} \tag{12}$$

for $\rho_T = P_T/\sigma_n^2$. Using (6), (9) and (12), it can be shown that for $\boldsymbol{e}_{\bar{\boldsymbol{\lambda}}_{\boldsymbol{k}}}^{(i)} = \hat{\bar{\boldsymbol{\lambda}}}_{i,k} - \bar{\boldsymbol{\lambda}}_{i,k}$, $\mathbf{E}_{k;k'} = \hat{\mathbf{H}}_{k;k'} - \mathbf{H}_{k;k'}$, and assuming that direct and image channels are uncorrelated i.e., $\mathbb{E}\{\boldsymbol{\Lambda}_{i,k}\boldsymbol{\Lambda}_{j,k'}^H\} \approx \mathbf{0},\ \forall\ i \neq j$, we have

$$\begin{aligned}\mathbf{R}_{\boldsymbol{\lambda}}^{(i)} &= \mathbb{E}\left\{\boldsymbol{e}_{\bar{\boldsymbol{\lambda}}_{\boldsymbol{k}}}^{(i)}\boldsymbol{e}_{\bar{\boldsymbol{\lambda}}_{\boldsymbol{k}}}^{(i)^H}\right\} \\ &= \mathbf{F}_M^H\mathbf{S}_k^T\mathbf{F}_{N,L}\mathbf{R}_{\boldsymbol{e}}^{(i)}\mathbf{F}_{N,L}^H\mathbf{S}_k\mathbf{F}_M \qquad (13)\\ \mathbf{R}_{\mathbf{E}} &= \mathbb{E}\left\{\mathbf{E}_{k;k'}\mathbf{E}_{k;k'}^H\right\} \\ &= \mathbf{F}_M^H\mathbf{S}_k^T\mathbf{F}_N\left(\mathbf{R}_{\mathbf{C}}^{(1)} + \mathbf{R}_{\mathbf{C}}^{(2)}\right)\mathbf{F}_N^H\mathbf{S}_k\mathbf{F}_M \qquad (14)\end{aligned}$$

where $[\mathbf{R}_{\mathbf{C}}^{(i)}]_{m,n} = \mathrm{Tr}\left\{\mathrm{diag}_{|m-n|}\left\{\mathbf{R}_{\boldsymbol{e}}^{(i)}\right\}\right\},\ \forall\ |m-n| \leq L$ and $[\mathbf{R}_{\mathbf{E}}]_{m,n} = \mathrm{Tr}\left\{\mathrm{diag}_{|m-n|}\left\{\mathbf{R}_{\bar{\boldsymbol{\lambda}}}^{(1)} + \mathbf{R}_{\bar{\boldsymbol{\lambda}}}^{(2)}\right\}\right\},\ \forall\ |m-n| \leq M$. In the following, we discuss some limiting cases for the error variance $\sigma_e^2 = \mathrm{Tr}\{\mathbf{R}_{\mathbf{E}}\}$ computation:

- *High SNR Regime:* When $\sigma_n^2 \to 0$, the channel estimator has diminishing error variance given by
$$\sigma_e^2 \approx 2L\rho_T^{-1} \to 0. \tag{15}$$
- *No IQI and Uniform normalized power delay profile (UN-PDP):* For $K \gg 1$, $L \geq M$ and when the pilot assignment is sufficiently spaced in frequency, the channel frequency snapshots observed by each user will be highly uncorrelated meaning, $\mathbb{E}\left\{\tilde{\boldsymbol{\lambda}}_{i,k}\tilde{\boldsymbol{\lambda}}_{i,k}^H\right\} = \sigma_H^2\mathbf{I}$, $\mathbf{R}_{\boldsymbol{e}}^{(1)} = \left(L\sigma_H^{-2} + \rho_T\right)^{-1}\mathbf{I}$ and $\mathbf{R}_{\boldsymbol{e}}^{(2)} = \mathbf{0}$. A simplification of (14) leads to,
$$\sigma_e^2 = \left(\sigma_H^{-2} + \frac{\rho_T}{L}\right)^{-1}. \tag{16}$$
When the channel coefficients have high correlation (e.g., $L \ll M$), σ_e^2 converges to (16) with $L \to 1$.
- *NFD IQI and UN-PDP:* $\mathbf{R}_{\boldsymbol{h}_k}^{(i)} = (\mu_i/L)\sigma_H^2\mathbf{I}$, $\mu_1 = |\alpha_{T,k}|^2|\alpha_R|^2 + |\beta_{T,k}|^2|\beta_R|^2$ and $\mu_2 = |\alpha_{T,k}|^2|\beta_R|^2 + |\beta_{T,k}|^2|\alpha_R|^2$. Then,
$$\sigma_e^2 = \left(\mu_1\sigma_H^{-2} + \frac{\rho_T}{L}\right)^{-1} + \left(\mu_2\sigma_H^{-2} + \frac{\rho_T}{L}\right)^{-1}. \tag{17}$$

III. Capacity Analysis

A. Ergodic Capacity

In this section, we provide a lower bound for the ergodic capacity $\mathcal{C}_{\mathrm{lo}}$ over all user (k, k') and subcarrier (m, m') pairs and considering the erroneous channel knowledge $\hat{\mathbf{H}}$.

Lemma 1: The lower bound on the instantaneous mutual information (IMI) with WLE receivers is given by

$$\mathcal{I}_{\mathrm{lo}}(\boldsymbol{y};\boldsymbol{x}|\hat{\mathbf{H}}) = \sum_{k=1}^{K/2}\sum_{m=1}^{M}\sum_{i=1}^{2}\log_2\left(1 + \frac{\mathcal{P}_{k,m}^{(i)}\lambda_{k,m}^{(i)}}{\bar{\sigma}_n^2}\right) \tag{18}$$

where $\lambda_{k,m}^{(i)}$ is the i-th singular-value of the Hermitian 2×2 matrix $\tilde{\mathbf{H}}_{k,m}^H\tilde{\mathbf{H}}_{k,m}$ with the effective channel as

$$\tilde{\mathbf{H}}_{k,m} = \begin{pmatrix}\tilde{\lambda}_{k,m}^{(1)} & \tilde{\lambda}_{k',m}^{(2)} \\ \tilde{\lambda}_{k,m'}^{(2)^*} & \tilde{\lambda}_{k',m'}^{(1)^*}\end{pmatrix} \tag{19}$$

and $\bar{\sigma}_n^2 = \sigma_n^2 + \sigma_e^2 P_D$ and $\mathcal{P}_{k,m}^{(i)}$ is the power assigned to the i-th sub-channel.

Proof: See Appendix A. ∎

Subject to the per-user sum power constraint and the stationarity assumptions on $\boldsymbol{h}_k$, the ergodic capacity is given by

$$\mathcal{C}_{\mathrm{lo}} = \frac{1}{K}\mathbb{E}_{\hat{\mathbf{H}}}\left\{\sup_{\forall\ k:\ \mathrm{Tr}\{\mathbf{Q}_k\}=P_D}\mathcal{I}_{\mathrm{lo}}(\boldsymbol{y};\boldsymbol{x}|\hat{\mathbf{H}})\right\} \tag{20}$$

In the case of no fading knowledge at the transmitter, the optimal input that maximizes (18) is i.i.d. over $\mathcal{S}_k$. Assuming small IQI such that

$$\lambda_{k,m}^{(i)} \approx \left|\tilde{\lambda}_{k,m}^{(1)}\right|^2 + \left|\tilde{\lambda}_{k,m'}^{(2)}\right|^2 \triangleq \mathcal{H}_{k,m} \tag{21}$$

and with $\bar{P}_D = P_D/M$, we have

$$\mathcal{C}_{\mathrm{lo}} \approx \frac{1}{K}\sum_{k=1}^{K}\sum_{m=1}^{M}\mathbb{E}_{\hat{\mathbf{H}}}\left\{\log_2\left(1 + \frac{\bar{P}_D\mathcal{H}_{k,m}}{\bar{\sigma}_n^2}\right)\right\}. \tag{22}$$

Proposition 1: When the channel $\boldsymbol{h}_k$ is Rayleigh distributed, the FD IQI parameters are deterministic and $\mathbb{E}\left\{\tilde{\lambda}_{k,m}^{(1)}\tilde{\lambda}_{k,m'}^{(2)^*}\right\} = 0$, the real RVs $\mathcal{H}_{k,m}$ have *generalized chi-squared distribution* with 2 degrees of freedom and the probability density function given as follows

$$p_{\mathcal{H}}(x) = \frac{\exp\left(-\frac{x}{\varsigma_{k,m}^{(1)}}\right) - \exp\left(-\frac{x}{\varsigma_{k,m}^{(2)}}\right)}{\varsigma_{k,m}^{(1)} - \varsigma_{k,m}^{(2)}},\ \forall\ x \geq 0, \tag{23}$$

and expectation can be obtained as

$$\mathbb{E}\left\{\mathcal{H}_{k,m}\right\} = \int_0^\infty x p_{\mathcal{H}}(x)\mathrm{d}x = \varsigma_{k,m}^{(1)} + \varsigma_{k,m}^{(2)} \triangleq \varsigma_{k,m} \tag{24}$$

where $\varsigma_{k,m}^{(1)} = \mathrm{var}\left\{\tilde{\lambda}_{k,m}^{(1)}\right\}$ and $\varsigma_{k,m}^{(2)} = \mathrm{var}\left\{\tilde{\lambda}_{k,m'}^{(2)}\right\}$.

Proof: See [13]. ∎

A comparison of the distribution of the exact eigenstructure and the approximate model is shown in Fig. 1. When the approximation seems to represent the actual channel accurately, a slight mismatch in the analytical distribution $p_{\mathcal{H}}(x)$ is expected due to the fact that $\tilde{\lambda}_{k,m}^{(1)}$ and $\tilde{\lambda}_{k,m'}^{(2)}$ are not entirely independent.

From proposition 1, the expectation operator in (22) can be explicitly stated as follows:

$$\mathcal{C}_{k,m} = \int_0^\infty \log_2\left(1 + \frac{\bar{P}_D x}{\bar{\sigma}_n^2}\right) p_{\mathcal{H}}(x)\mathrm{d}x \tag{25}$$

$$= \frac{\log_2 e}{\left(\varsigma_{k,m}^{(1)} - \varsigma_{k,m}^{(2)}\right)}\left(\exp\left(\varrho_{k,m}^{(2)}\right)\mathrm{Ei}\left(-\varrho_{k,m}^{(2)}\right) - \exp\left(\varrho_{k,m}^{(1)}\right)\mathrm{Ei}\left(-\varrho_{k,m}^{(1)}\right)\right) \tag{26}$$

where

$$\varrho_{k,m}^{(i)} = \frac{\bar{\sigma}_n^2}{\varsigma_{k,m}^{(i)}\bar{P}_D} \text{ and } \mathrm{Ei}(x) = \int_{-\infty}^{x} \frac{\exp(t)}{t}\mathrm{d}t. \tag{27}$$

Note that if we disregard $\bar{\sigma}_n^2$, then increasing $\varsigma_{k,m}^{(2)}$ but strictly $\varsigma_{k,m}^{(2)} < \varsigma_{k,m}^{(1)}$ (holds for practical IQI) and fixing $\varsigma_{k,m} = \varsigma_{k,m}^{(1)} + \varsigma_{k,m}^{(2)}$, the gap between terms in (26) narrows down that results in an overall capacity reduction even with a slightly larger scaling factor. It implies that WLE cannot exceed the capacity bound of the ideal linear equalizers (LEs). At high SNR $P_{k,m}\mathcal{H}_{k,m} \gg \sigma_n^2 + \sigma_e^2 P_D$, the uniform power allocation (UPA) is indeed optimal and (25) can be rewritten as

$$\mathcal{C}_{k,m} = \log_2\left(\frac{\bar{P}_D}{\bar{\sigma}_n^2}\right) + \mathbb{E}_{\hat{\mathbf{H}}}\left\{\log_2 \mathcal{H}_{k,m}\right\} = \log_2\left(\frac{\bar{P}_D}{\bar{\sigma}_n^2}\right) + \frac{1}{\ln 2}\cdot\left[\frac{\varsigma_{k,m}^{(1)}\ln\varsigma_{k,m}^{(1)} - \varsigma_{k,m}^{(2)}\ln\varsigma_{k,m}^{(2)}}{\varsigma_{k,m}^{(1)} - \varsigma_{k,m}^{(2)}} - C\right] \tag{28}$$

where C is Euler's constant. In the low SNR region, the function $\log_2(1+gx)$ with $x > 0$ and small $g(\mathrm{SNR})$ gives,

$$\mathcal{C}_{k,m} = \frac{\bar{P}_D \varsigma_{k,m}}{\ln 2 \cdot \bar{\sigma}_n^2} + \mathcal{O}\left(g^2\right). \tag{29}$$

The results (22)-(29) are intuitively appealing as:

- They converge to the classical capacity expressions with LE receivers (e.g., [5]) in the absence of IQI (with $\varsigma_{k,m}^{(2)} \to 0$ in (26) and $\mathbf{R}_{\mathbf{e}}^{(2)} = \mathbf{0}$ in (12)).
- Asymptotic ergodic capacity $\mathcal{C}_{k,m}$ grows unbounded in SNR as $\sigma_e^2 \to 0$ in (15). Nonetheless, if $P_T \ll P_D$, then from (16) and (17), the effective SNR is bounded by ρ_T. This accentuates the importance of obtaining reliable channel estimates (11), such that $\sigma_e^2 P_D \ll \sigma_n^2$.
- The user specific estimation error (14), the SNR scaling in (26) and the capacity offset in (28) realize the IQI influence. In other words, capacity relates to the IQI problem through the variance of the components of the effective channel $\mathcal{H}_{k,m}$, the extent of the CSI knowledge[2] and its error variance σ_e^2.

If the transmitter knows the frequency-selective fading coefficients via a reliable feedback channel, then it can choose the input covariance matrix $\mathbf{Q}_{k;k'}$ as function of $\hat{\mathbf{H}}_{k;k'}$ in order to maximize the mutual information. This leads to a well-known water-filling power allocation (WPA) functions as follows:

$$\mathcal{P}_{k,m} = \left[\nu_k - \frac{\bar{\sigma}_n^2}{\mathcal{H}_{k,m}}\right]^+ \tag{30}$$

giving $\mathcal{P}_{k,m} \geq 0,\ \forall\ k,m$. The water-level ν_k is chosen such that the maximum instantaneous transmit power satisfies the constraint $\sum_{m=1}^{M}\mathcal{P}_{k,m} = P_D,\ \forall\ k$. Equation (30) shows that a change in the effective channel $\mathcal{H}_{k,m}$ structure could shift the distribution of the power between the desired and the image band. In fact, the power allocation scheme (30) is similar to the classical capacity maximizing water-filling scheme, except that here spectrum shaping gives more weightage to the stronger direct and image channel pairs.

B. Outage Capacity

The event of outage on the k-th user link occurs if the user IMI $\mathcal{I}_k = \sum_m \mathcal{I}_{k,m}$ from (18) drops below a certain threshold γ:

$$P_{out}(k) = Pr\left(\mathcal{I}_k < \gamma\right). \tag{31}$$

In order to characterize the outage probability, the PDF of $\mathcal{I}_k$ is required. As seen from (18), the user IMI $\mathcal{I}_k$ is a summation over $\mathcal{S}_k$ frequency resources. For practical $N \gg 1$ and i.i.d. RVs $\mathcal{H}_{k,m}, \mathcal{I}_k$ approximately follows a Gaussian distribution sufficiently described by its first two moments i.e., $\mathcal{I}_k \sim \mathcal{N}\left(\bar{\mathcal{C}}_k, \sigma_{C_k}^2\right)$ [14]. From (26), we have $\bar{\mathcal{C}}_k = \sum_m \mathcal{C}_{k,m}$. As for the variance of the sum of user's IMIs, we note that

$$\sigma_{C_k}^2 = \mathbb{E}_{\hat{\mathbf{H}}}\left\{\left(\mathcal{I}_k - \bar{\mathcal{C}}_k\right)^2\right\} = 2\sum_{m=1}^{M}\sum_{n>m}\mathbb{E}_{\hat{\mathbf{H}}}\left\{\mathcal{I}_{k,m}\mathcal{I}_{k,n}\right\} - \bar{\mathcal{C}}_k^2. \tag{32}$$

[2] If only the direct channel is known, then the variance of the off-diagonal terms in $\tilde{\mathbf{H}}_{k,m}$ should be diverted to σ_e^2 leading to an asymptotically finite rate in (28).

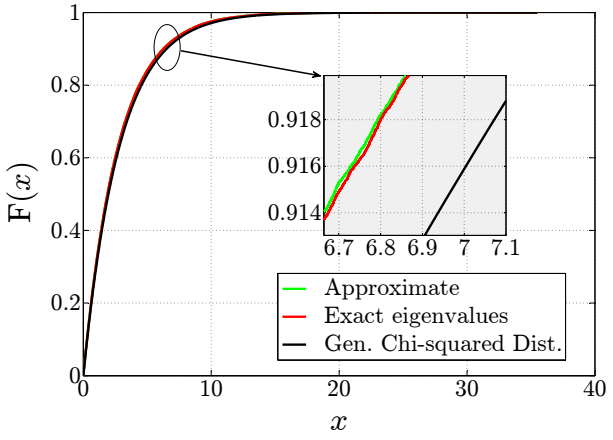

Fig. 1: CDF of the effective channel eigenvalue $\lambda_{k,m}^{(i)}$ and its approximation $\mathcal{H}_{k,m}$ for a reference scenario (see Sec. IV).

The above expression depends on the cross-correlation of the individual IMIs $\mathcal{M}_{k,m,n} = \mathbb{E}_{\tilde{\mathbf{H}}}\{\mathcal{I}_{k,m}\mathcal{I}_{k,n}\}$ that are a function of the channel power gains $\mathcal{H}_{k,m}$ and $\mathcal{H}_{k,n}$. The exact computation of (32) requires the PDF of RV's nonlinear transformation that is in general difficult to derive. Thus, here we resort to an approximate solution by truncating the Taylor series into a function of the RV's moments around $\mathbb{E}\{\mathcal{H}_{k,m}\}$ as in [15]:

$$\sigma_{C_k}^2 \approx 2\sum_{m=1}^{M}\sum_{n>m}\frac{\partial \mathcal{I}_k}{\partial \mathcal{H}_{k,m}}\frac{\partial \mathcal{I}_k}{\partial \mathcal{H}_{k,n}}\mathrm{cov}\{\mathcal{H}_{k,m},\mathcal{H}_{k,n}\} \quad (33)$$

where the partial derivatives $\partial\mathcal{I}_k/\partial\mathcal{H}_{k,m}$ are evaluated at $\mathbb{E}\{\mathcal{H}_{k,m}\}$ and thus give

$$\left.\frac{\partial \mathcal{I}_k}{\partial \mathcal{H}_{k,m}}\right|_{\mathbb{E}\{\mathcal{H}_{k,m}\}} = \frac{\ln 2}{\bar{\sigma}_n^2+\sigma_{\mathcal{H}}^2}. \quad (34)$$

Moreover, from the definition of $\mathcal{H}_{k,m}$, the covariance $c_{m,n}^k = \mathrm{cov}\{\mathcal{H}_{k,m},\mathcal{H}_{k,n}\}$ computation results in

$$c_{m,n} = \varsigma_{k,m,n}^{(1,1)} + \varsigma_{k,m,n}^{(2,2)} + \varsigma_{k,m,n}^{(1,2)} + \varsigma_{k,m,n}^{(2,1)} - \varsigma_{k,m}\varsigma_{k,n} \quad (35)$$

where $\varsigma_{k,m,n}^{(q,p)} = \mathbb{E}\left\{\left|\tilde{\lambda}_{k,m}^{(p)}\right|^2\left|\tilde{\lambda}_{k,n}^{(q)}\right|^2\right\}$. Finally, the outage probability is obtained as

$$P_{out}(k) = 1 - \mathcal{Q}\left\{\frac{\gamma-\bar{\mathcal{C}}_k}{\sigma_{C_k}}\right\} \quad (36)$$

where $\mathcal{Q}\{\cdot\}$ is the standard Q-function. From (36), it is clear that the outage probability is influenced by the IQI and the channel correlation through the variance of IMI (34) and decreases monotonically with decreasing $\sigma_{C_k}^2$ given $\bar{\mathcal{C}}_k > \gamma$, as $\bar{\mathcal{C}}_k$ is not profoundly affected by the spectral correlations. In the absence of IQI, the deciding factor is the covariance of the power gains $\left|\tilde{\lambda}_{k,m}^{(1)}\right|^2$ and $\left|\tilde{\lambda}_{k,n}^{(1)}\right|^2$, whose range could be specified for Rayleigh fading channels as $1 \geq \mathrm{cov}\left\{\left|\tilde{\lambda}_{k,m}^{(1)}\right|^2,\left|\tilde{\lambda}_{k,n}^{(1)}\right|^2\right\}/\sigma_H^4 = \left|\rho_{n,m}^k\right|^2 \geq 0$, where $\rho_{n,m}^k = \mathbb{E}\left\{\tilde{\lambda}_{k,m}^{(1)}\tilde{\lambda}_{k,n}^{(1)^*}\right\}$. Its lower bound explains the frequency diversity achieved by de-correlating channels via interleaved subcarrier assignment [10], whereas the upper bound indicates that the capacity outage events cannot be avoided in a highly correlated channel. The presence of IQI elevates the value of $c_{m,n}^k$ by intra-user channel correlation terms. Its minimum is achieved when $\rho_{n,m}^k \to 0$ and $\varsigma_{k,m,n}^{(p,q)} \to 0,\ \forall\ p \neq q$ in (35). One possible way to achieve this is to map the direct-image pair (s_m, s_n) to different users i.e., if $s_m \in \mathcal{S}_k$, then $N - s_n \notin \mathcal{S}_k$. Interestingly for single tap linear equalizer (LEs), the later condition is opposite i.e., $\mathbb{E}\left\{\tilde{\lambda}_{k,m}^{(1)}\tilde{\lambda}_{k',m}^{(2)^*}\right\} \neq 0$ leading to $k = k'$ [16].

Proposition 2: If the channel coefficients $\tilde{\boldsymbol{\lambda}}_{1,k}$ are independent[3] and have the same distribution[4], then the variance $\sigma_{C_k}^2$ of the mutual information $\mathcal{I}_k$ given in (32) can be computed in closed form as

$$\begin{aligned}\sigma_{C_k}^2 = \left(\frac{M\log_2 e}{\varsigma_k^{(1)}-\varsigma_k^{(2)}}\right)^2\Bigg[&\frac{\pi^2}{6}\left(e^{\zeta_k^{(1)}}\varsigma_k^{(1)} - e^{\zeta_k^{(2)}}\varsigma_k^{(2)}\right)\\ &+ e^{\zeta_k^{(1)}}\varsigma_k^{(1)}\left(C+\ln\zeta_k^{(1)}\right)^2\\ &- e^{\zeta_k^{(2)}}\varsigma_k^{(2)}\left(C+\ln\zeta_k^{(2)}\right)^2\Bigg] - \bar{\mathcal{C}}_k^2\end{aligned} \quad (37)$$

where $\zeta_k^{(i)} = \frac{\bar{\sigma}_n^2}{\bar{P}_D\varsigma_k^{(i)}}$.

Proof: Rewriting $\mathcal{M}_{k,m,n}|_{m=n}^{\mathrm{NFD}} = \mathcal{M}_k$ in (32) using (23), (21) and (18), we have

$$\begin{aligned}\mathcal{M}_k &= \int_0^\infty\left(\log_2\left(1+\frac{\bar{P}_D x}{\bar{\sigma}_n^2}\right)\right)^2 p_{\mathcal{H}}(x)\mathrm{d}x\\ &= \left(\frac{M}{\varsigma_k^{(1)}-\varsigma_k^{(2)}}\right)^2\Bigg[\int_0^\infty\left(\log_2\left(1+\frac{\bar{P}_D x}{\bar{\sigma}_n^2}\right)\right)^2 e^{-\frac{x}{\varsigma_k^{(1)}}}\mathrm{d}x\\ &\quad - \int_0^\infty\left(\log_2\left(1+\frac{\bar{P}_D x}{\bar{\sigma}_n^2}\right)\right)^2 e^{-\frac{x}{\varsigma_k^{(2)}}}\mathrm{d}x\Bigg]\end{aligned} \quad (38)$$

Next making the substitution $y = 1+\bar{P}_D x/\bar{\sigma}_n^2$ and exploiting the following relation [17]:

$$\int_0^\infty(\ln y)^2 e^{-\mu y}\mathrm{d}y = \frac{1}{\mu}\left(\frac{\pi^2}{6}+(C+\ln\mu)^2\right) \quad (39)$$

leads to (37). ■

[3]This assumption ensures that, in the case of TX IQI, the direct $\tilde{\lambda}_{k,m}^{(1)}$ and image $\tilde{\lambda}_{k,m'}^{(2)}$ channels of the k^{th} user are independent, since the image channel $\tilde{\lambda}_{k,m'}^{(2)}$ corresponds to the scaled channel realization i.e., $\tilde{\boldsymbol{\lambda}}_k^{(2)}$ sampled at a different frequency location (unless $s_m \in \{0, N/2\}$).

[4]Assuming that IQI is NFD, from (5) it is obvious that the entries of $\tilde{\boldsymbol{\lambda}}_k^{(i)}$ will be independent and have the same variance $\varsigma_k^{(i)}$.

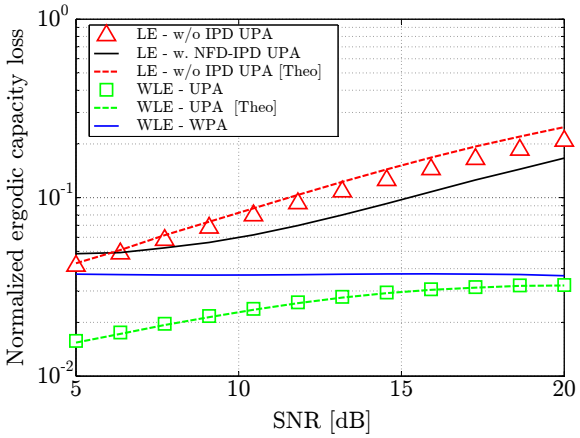

Fig. 2: Achievable user rate loss w.r.t the ideal system for different schemes and interleaved assignment.

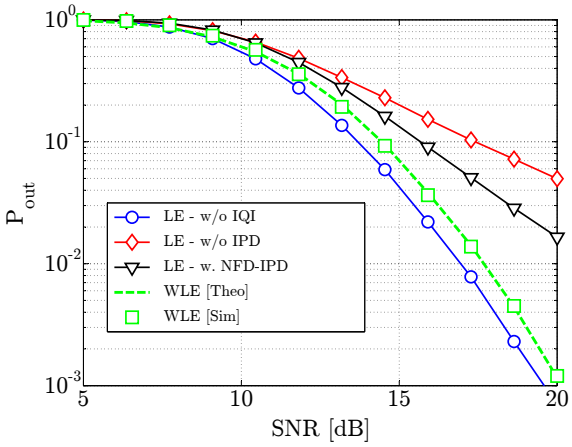

Fig. 4: Outage probability for various schemes against SNR: Outage capacity $\mathcal{C}_k \geq 128$ bits per channel use and evaluated for the first user in an interleaved assignment.

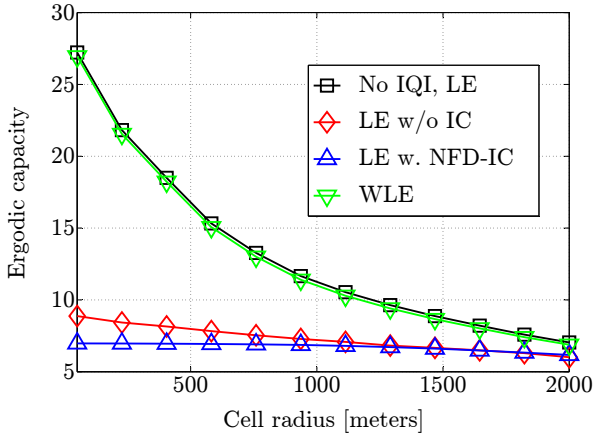

Fig. 3: User ergodic capacity per subcarrier as a function of the cell size for interleaved assignment: $f_c = 1800$ MHz, $W = 10$ MHz, $NF = 9$ dB and $P_t = 1$ mW.

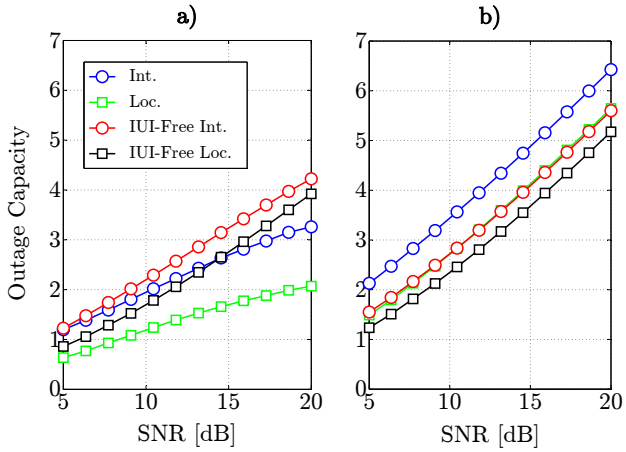

Fig. 5: Outage capacity $\mathcal{C}_k = \bar{\mathcal{C}}_k/M$ of WLE for an outage probability $P_{out} \leq 10^{-2}$.

Although not explicitly shown here, the asymptotic convergence ($\sigma_n^2 \rightarrow 0$) of $\mathcal{M}_k$ to $\bar{\mathcal{C}}_k^2$ in (28) is evident. This implies that the outage probability will vanish at high SNR. Also interestingly, as $\varsigma_k^{(2)} \rightarrow \varsigma_k^{(1)}$, an increase in $\sigma_{\bar{C}_k}^2$ is observed in (37) that reduces P_{out} and is further aggravated by slight degradation in the ergodic capacity $\bar{\mathcal{C}}_k$ as mentioned in Section III-A.

IV. Numerical Analysis

In this section, we present simulation results for a reference LTE SC-FDMA system with the following parameter set (unless otherwise stated explicitly) :$K = 4$, $M = 32$, $N = 256$ and maximum used subcarriers $N_u = 200$. Note that due to the null DC tone, the user relationships identified in [5] does not hold and in IUI assignments (localized or interleaved), each user suffers with interference from a different user irrespective of its position i.e, for both assignment types ❶$\overset{\text{IUI}}{\leftrightarrow}$❹ and ❷$\overset{\text{IUI}}{\leftrightarrow}$❸. The FIR channels $\boldsymbol{h}_k$ were simulated with complex Gaussian i.i.d taps having exponential power delay profile $\sigma_l^2 = c\exp(-l/\sigma_{rms})$, $\forall\, l \in [0\ L-1]$ with $L = 8$ and c such that $\sum_l \sigma_l^2 = 1$. As IQI is expected to be a dominantly TX side impairment in an uplink system, we considered the TX IQI only. The IQI parameters are pre-defined with slightly different image-rejection ratios

$$\text{ILR}_k(m) \triangleq \frac{\left|\mathbf{F}_{m,M}^H \mathbf{S}_{k'}^T \mathbf{F}_N \boldsymbol{g}_{2T,k'}\right|}{\left|\mathbf{F}_{m,M}^H \mathbf{S}_k^T \mathbf{F}_N \boldsymbol{g}_{1T,k}\right|} \tag{40}$$

and $\text{ILR}_k = (1/M)\sum_m \text{ILR}_k(m)$ as $\{-18.7,\ -17.3,\ -19.5,\ -18.8\}$ dB, except in Fig. 6 when all users have same $\text{ILR}_k = -18.7$ dB.

The ergodic capacity loss of LE and WLE receivers are depicted in Fig. 2. We observe that UPA WLE receiver approaches a constant throughput loss at high SNR. One possible reason is that the additional error penalty due to the dual channel model leads to higher capacity loss at high SNRs. However in WPA as the erroneous CSI is used for water-filling power allocation, this effect is uniform over a broad SNR range. On the other hand, LE receiver suffers from the image interference problem. Also shown is the NFD interference pre-distortion (IPD) that provides an improvement of around 6%.[5,6] The user capacity is asymptotically unbounded as estimation error vanishes for high SNRs. Analytical results predict the capacity behavior accurately, except for the LE receivers, in which case Jensen's approximate of capacity expression results in an underestimate of the capacity at high SNRs. In order to analyze the relationship between net throughput and coverage, we use the path loss model specified in [12] and place all users equi-distant from the base station. It is obvious from Fig. 3 that WLE could extend cellular coverage to within 15 meters of the ideal UEs whereas coverage is considerably reduced with LE and NFD-IPD receivers.

The outage performance with the static power control is provided in Fig.4, when the target sum user rate is $\mathcal{C}_k \geq 128$ bits per channel use for NFD IQI. It is shown that the analytical formulation (36) provides quite a good estimate on P_{out} in WLE receivers. In addition, it is shown that WLE suffers a performance degradation of around 1 dB. Moreover, by the slopes of the curves, it can be concluded that the system diversity is higher for WLE. In both receivers, the image channel $\tilde{\lambda}_{k,m}^{(2)}$ strengthens the effective channel $\mathcal{H}_{k,m}$, when the direct channel $\tilde{\lambda}_{k,m}^{(1)}$ is in deep fade but WLE exploits it better by tracking actual image profile $\bar{\boldsymbol{\lambda}}_k^{(2)}$, whereas NFD IPD realizes it by its zeroth-order estimate.

From Fig. 5, it is seen that in general, the interleaved schemes performs better than the localized versions from the outage perspective as more diversity is manifested by the former. Interestingly, IUI is beneficial for WLEs, whereas IUI-free schemes increase the outage capacity of the LE. These results should be interpreted with caution, since in addition to the uncorrelated channel requirements, the outage capacity will be higher for IUI-free schemes if $\mathrm{ILR}(\textcircled{k} \to \textcircled{k}) \gg \mathrm{ILR}(\textcircled{k} \to \textcircled{k'})$, $\forall\, k \neq k'$, contrary to a LE receiver which suffers degradation from its image user and an improvement is possible when $\mathrm{ILR}(\textcircled{k'} \to \textcircled{k}) \gg \mathrm{ILR}(\textcircled{k} \to \textcircled{k})$, $\forall\, k \neq k'$.

In Fig. 6, we compare the outage capacity of a user for different configurations but fixed resources per user. With increasing K, user achieves a higher capacity region because it experiences greater user separation in frequency making higher diversity achievable. On the other hand, reducing the frequency resolution (fixed sampling rate) has adverse effect on the capacity, since the channel coefficient correlation $\rho_{m,n}^k$ increases when more subcarriers are packed in the same bandwidth. As the frequency-selectivity of the channel decreases, the outage events become common leading to a lower throughput.

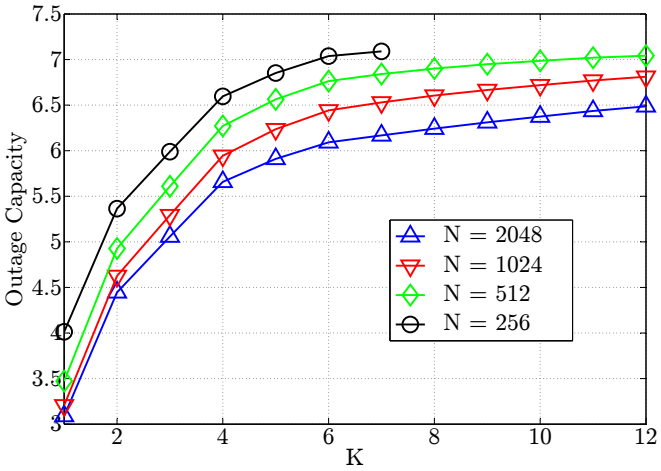

Fig. 6: Outage capacity of WLE for different user and resource configurations: Outage probability $P_{out} \leq 10^{-2}$, $M = 32$, SNR $= 20$ dB and interleaved assignment.

V. Conclusions

In this paper, we have analyzed the capacity of a MU system affected by the IQI and the channel estimation error. We derived the error covariance matrix for the CSI required by the WLE receivers. Using the imperfect CSI knowledge, the ergodic and outage capacity of a multi-user network were stated in a closed form under some given conditions. As the WLE receiver was able to compensate for the interference due to IQI and the channel estimation error diminishes with SNR, the ergodic capacity grows unbounded asymptotically. For the outage performance, the channel correlation was found to have detrimental impact on WLE performance. Finally, we established the merits of the WLE receivers using the subcarrier assignment schemes adopted in 3GPP LTE standard as well as their IUI-free counterparts.

Appendix A
Lower Bound on Mutual Information

When LMMSE channel estimation is used, the model (8) can be written as

$$\boldsymbol{y}_{k;k'} = \hat{\mathbf{H}}_{k;k'}\boldsymbol{x}_{k;k'} + \mathbf{E}_{k;k'}\boldsymbol{x}_{k;k'} + \boldsymbol{w}_{k;k'} \qquad (41)$$

where the second and third terms constitute the effective noise contribution and the entries of $\hat{\mathbf{H}}_{k;k'}$ and $\mathbf{E}_{k;k'}$ are

[5]Different from [3] that considers RX IQI, in our scenario the TX IQI cannot be canceled at the receiver judging from (5). Therefore, likelihood function [4] for joint channel $\boldsymbol{h}_k$ and IQI IPD μ_k estimation is realized with IQI pre-distortion i.e., $\Lambda\left(\boldsymbol{h}_k, \mu_k\right) = -\|\boldsymbol{y}_k - \left(\mathbf{U}_k + \mu_k \mathbf{U}_k^*\right)\boldsymbol{h}_k\|^2$, where $\mu_k = \beta_{T,k}/\alpha_{T,k}^*$.

[6]Estimation of FD IPD requires blind adaptive techniques [18] that exploit signal statistical properties for parameter resolution. However, in the presence of high IQI, it is difficult to separate FD IQI parameters from the propagation channel. Thus, here we restrict IPD scheme to NFD IQI mitigation.

independent. Following similar steps as in [19] and with optimal linear equalizers in (7), we have

$$\begin{aligned}\mathcal{I}(\boldsymbol{y};\boldsymbol{x}|\hat{\mathbf{H}}) &\geq \frac{1}{2}\log_2 \det\left|\mathbf{I}+\hat{\mathbf{H}}^H\left(\mathbf{R}_{\boldsymbol{w}}+\mathbf{E}\mathbf{Q}\mathbf{E}^H\right)^{-1}\hat{\mathbf{H}}\mathbf{Q}\right| \\ &\overset{(a)}{\approx} \sum_{k=1}^{K/2}\log_2 \det\Big|\mathbf{I}+\hat{\mathbf{H}}_{k;k'}^H \\ &\quad\times\left(\mathbf{R}_{\boldsymbol{w}_{k;k'}}+\mathbf{E}_{k;k'}\mathbf{Q}_{k;k'}\mathbf{E}_{k;k'}^H\right)^{-1}\hat{\mathbf{H}}_{k;k'}\mathbf{Q}_{k;k'}\Big| \\ &\overset{(b)}{\approx} \sum_{k=1}^{K/2}\log_2 \det\left|\mathbf{I}+\left(\sigma_n^2+\sigma_e^2 P_D\right)^{-1}\tilde{\boldsymbol{\Sigma}}_{k;k'}\tilde{\mathbf{Q}}_{k;k'}\right|.\end{aligned}$$

In step (a), the inter-user noise correlation due to RX IQI is ignored and it is assumed that the last $K/2$ users lie in the image band of the first $K/2$ users. Step (b) results by diagonalizing the noise covariance matrices, and assuming further that

$$\mathbb{E}\left\{\mathbf{E}_{k;k'}\boldsymbol{x}_{k;k'}\boldsymbol{x}_{k;k'}^H\mathbf{E}_{k;k'}^H\right\}\approx\sigma_e^2(P_D/M)\mathbf{I} \qquad (42)$$

which holds considering (14) and in high SNR, when all resources are active $\mathcal{P}_{k,m}^{(i)}\neq 0,\forall\ k,m,i$. The dual-channel matrix can be decomposed using singular-value decomposition as

$$\hat{\mathbf{H}}_{k;k'}=\mathbf{U}_{k;k'}\mathbf{D}_{k;k'}\mathbf{V}_{k;k'}^H \qquad (43)$$

yielding $\tilde{\boldsymbol{\Sigma}}_{k;k'}=\mathbf{D}_{k;k'}^H\mathbf{D}_{k;k'}$ and $\tilde{\mathbf{Q}}_{k;k'}=\mathbf{V}_{k;k'}^H\mathbf{Q}_{k;k'}\mathbf{V}_{k;k'}$. The fact that $\mathbf{U}_{k;k'}$ and $\mathbf{V}_{k;k'}$ are unitary matrices leads to (18).

REFERENCES

[1] H. Myung, J. Lim, and D. Goodman, "Single carrier FDMA for uplink wireless transmission," *IEEE Veh. Technol. Mag.*, vol. 1, no. 3, pp. 30–38, 2006.

[2] A. Ismail and A. Abidi, "A 3.1- to 8.2-GHz zero-IF receiver and direct frequency synthesizer in 0.18- μm SiGe BiCMOS for mode-2 MB-OFDM UWB communication," *IEEE Trans. Syst. Sci. Cybern.*, vol. 40, no. 12, pp. 2573–2582, 2005.

[3] Y.-H. Chung and S.-M. Phoong, "Joint estimation of I/Q imbalance, CFO and channel response for MIMO OFDM systems," *IEEE Trans. Commun.*, vol. 58, no. 5, pp. 1485–1492, 2010.

[4] G.-T. Gil, I.-H. Sohn, J.-K. Park, and Y. H. Lee, "Joint ML estimation of carrier frequency, channel, I/Q mismatch, and DC offset in communication receivers," *Vehicular Technology, IEEE Transactions on*, vol. 54, no. 1, pp. 338–349, 2005.

[5] Y. Yoshida, K. Hayashi, H. Sakai, and W. Bocquet, "Analysis and compensation of transmitter IQ imbalances in OFDMA and SC-FDMA systems," *IEEE Trans. Signal Process.*, vol. 57, no. 8, pp. 3119–3129, 2009.

[6] B. Narasimhan, S. Narayanan, H. Minn, and N. Al-Dhahir, "Reduced-complexity baseband compensation of joint Tx/Rx I/Q imbalance in mobile MIMO-OFDM," *IEEE Trans. Wireless Commun.*, vol. 9, no. 5, pp. 1720–1728, 2010.

[7] H. Minn and D. Munoz, "Pilot designs for channel estimation of MIMO OFDM systems with frequency-dependent I/Q imbalances," *IEEE Trans. Commun.*, vol. 58, no. 8, pp. 2252–2264, 2010.

[8] S. Krone and G. Fettweis, "Capacity analysis for OFDM systems with transceiver I/Q imbalance," in *Global Telecommunications Conference, 2008. IEEE GLOBECOM 2008. IEEE*, 2008, pp. 1–6.

[9] S. Song, G. Chen, and K. Letaief, "Localized or interleaved? a trade-off between diversity and CFO interference in multipath channels," *IEEE Trans. Wireless Commun.*, vol. 10, no. 9, pp. 2829–2834, 2011.

[10] T. Svensson, T. Frank, D. Falconer, M. Sternad, E. Costa, and A. Klein, "B-IFDMA - a power efficient multiple access scheme for non-frequency-adaptive transmission," in *Mobile and Wireless Communications Summit, 2007. 16th IST*, 2007, pp. 1–5.

[11] D. Darsena, G. Gelli, L. Paura, and F. Verde, "Widely linear equalization and blind channel identification for interference-contaminated multicarrier systems," *IEEE Trans. Signal Process.*, vol. 53, no. 3, pp. 1163–1177, 2005.

[12] "Physical layer aspects for evolved universal terrestrial radio access (UTRA)," *3GPP TR 25.814 V7.1.0 (2006-09)*.

[13] D. Hammarwall, M. Bengtsson, and B. Ottersten, "Acquiring partial CSI for spatially selective transmission by instantaneous channel norm feedback," *IEEE Trans. Signal Process.*, vol. 56, no. 3, pp. 1188–1204, 2008.

[14] H. Boostanimehr and V. Bhargava, "Outage capacity analysis for OFDM decode-and-forward systems in frequency selective rayleigh fading channels," *IEEE Commun. Lett.*, vol. 16, no. 6, pp. 937–940, 2012.

[15] S. O. Rice, "Mathematical analysis of random noise," in *Bell Syst. Tech. J.*, vol. 24, 1945, pp. 44–156.

[16] A. Gomaa and N. Al-Dhahir, "Multi-user SC-FDMA systems under IQ imbalance: EVM and subcarrier mapping impact," in *Global Telecommunications Conference (GLOBECOM 2011), IEEE*, 2011, pp. 1–5.

[17] I. Gradshteyn and I. Ryzhik, "Table of Integrals, Series, and Products," *Academic Press*, 2007.

[18] L. Anttila, M. Valkama, and M. Renfors, "Circularity-based I/Q imbalance compensation in wideband direct-conversion receivers," *IEEE Trans. Veh. Technol.*, vol. 57, no. 4, pp. 2099–2113, 2008.

[19] T. Yoo and A. Goldsmith, "Capacity and power allocation for fading mimo channels with channel estimation error," *Information Theory, IEEE Transactions on*, vol. 52, no. 5, pp. 2203–2214, 2006.